Diffusion-limited and advection-driven electrodeposition in a microfluidic channel

A. Wlasenko,[1] F. Soltani,[1] D. Zakopcan,[1] D. Sinton,[2] and G. M. Steeves[1]

[1]*Department of Physics and Astronomy, University of Victoria, P.O. Box 3055, STN CSC, Victoria, British Columbia, Canada V8W 3P6*

[2]*Department of Mechanical Engineering, University of Victoria, P.O. Box 3055, STN CSC, Victoria, British Columbia, Canada V8W 3P6*

(Received 30 September 2009; published 1 February 2010)

Self-terminating electrochemical fabrication was used within a microfluidic channel to create a junction between two Au electrodes separated by a gap of 75 μm. During the electrochemical process of etching from the anode to deposition at the cathode, flow could be applied in the anode-to-cathode direction. Without applied flow, dendritic growth and dense branching morphologies were typically observed at the cathode. The addition of applied flow resulted in a densely packed gold structure that filled the channel. A computer simulation was developed to explore regimes where the diffusion, flow, and electric field between the electrodes individually dominated growth. The model provided good qualitative agreement relating flow to the experimental results. The model was also used to contrast the effects of open and closed boundaries and electric field strength, as factors related to tapering.

DOI: 10.1103/PhysRevE.81.021601 PACS number(s): 68.70.+w, 82.45.Qr, 47.60.−i, 61.43.Hv

I. INTRODUCTION

Techniques to fabricate and manipulate electronic systems with precision on the scale of a nanometer are crucial in such fields as nanoelectronics and chemical sensing. Connected and unconnected electrodes have been created on the nanoscale using such techniques as scanning probe microscopy [1–17], mechanically controllable break junctions [18–27], electron beams [28–35], electromigration [36–42], and electrochemistry [43–58]. Using electrochemistry, complex growth between macroscopic electrodes can culminate in simple nanoscale junctions. These junctions function as reliable quantum point contacts, however the electrochemical fabrication approach introduces large variance in the formation and location of individual junctions. Understanding and controlling this process will enable the precise positioning of reproducible geometries into nanoelectronic devices.

In the electrochemical approach of Boussaad and Tao [46], two macroscopic electrodes, separated by a 20 μm wide gap, were placed in series with a load resistor as a bias voltage (V_0) was applied. An electrolytic solution covered the gap and the voltage across the electrodes (V) induced etching from the anode and electrodeposition at the cathode. As the cathode grew into contact with the anode, the resistance (R) decreased leading to a reduction in V,

$$V = \frac{R}{R + R_L} V_0, \quad (1)$$

where R_L is the resistance of the load. The electrochemical rate is affected by V, thus the current density (J), according to the Butler-Volmer equation

$$J = J_0\left[\exp\left(\frac{\alpha_a eV}{k_B T}\right) - \exp\left(-\frac{\alpha_c eV}{k_B T}\right)\right], \quad (2)$$

where J_0 is exchange current density, α_a and α_c are the anodic and cathodic transfer coefficients, respectively, e is the charge of the electron, k_B is Boltzman's constant, and T is the temperature. This exponential dependence on V leads to a self-termination effect in the formation of the junction as the electrochemical reaction at the junction effectively halts. By choosing $1/R_L$ near to the quantum of conductance ($G_0 = 2e^2/h \approx 1/12.9$ kΩ), one can select the formation of quantum point contacts [46].

II. EXPERIMENTAL SETUP AND PRELIMINARY OBSERVATIONS

This work was extended by confining the electrochemistry within a microfluidic channel. Others have used microfluidic channels perpendicular to the electrodes to rinse the junction for reuse after contact was made between the electrodes, however no flow was applied during formation in that case [55]. In the experiment developed here, flow is applied during the deposition process in the anode-to-cathode direction in an effort to influence ion transport. As an additional control parameter, applied flow has the advantage that it is independent of the electrode geometry and applied voltage to which ion migration and electrochemistry are coupled.

The channels were patterned in a 2-mm-thick layer of polydimethylsiloxane (PDMS) and fabricated using soft-lithography microfabrication methods [59]. The PDMS contained an array of microchannels running parallel to one another that were several cm long, 30 μm high, and 200 μm wide. Au-coated glass slides (100 nm of Au, 20 nm of Cr, from the Evaporated Metal Films Corporation) were etched to produce gold electrodes with 75 μm gaps between them. The microchannels were aligned over the electrodes, and a Plexiglas coverplate and a clamp provided a mechanical seal between the PDMS and the glass substrate. Figure 1(a) shows the experimental setup. The fluid flow was controlled using a Harvard Compact Infusion Pump Model 975 (analog motor control) to infuse a solution of 2M HCl into the microchannels. The Au electrodes were connected in series with a load resistor (50 kΩ) to a current amplifier that monitored when the electrodes had come into electrical contact. Examples of scanning electron microscope (SEM) images of deposits that were created with the setup are shown for the

 ©2010 The American Physical Society

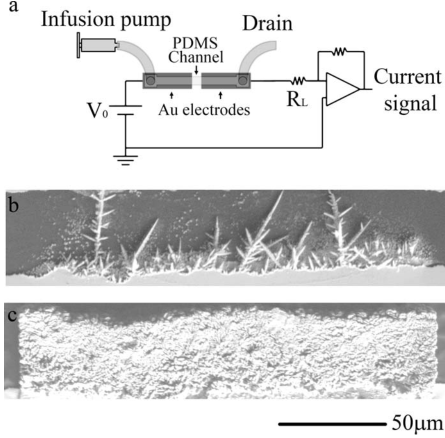

FIG. 1. (a) Schematic of experimental setup. Ion flow is controlled in the PDMS channel during electrodeposition between the gold electrodes and a current amplifier monitors when the process self-terminates. Examples of SEM images of deposition across roughly 40 μm of the electrode gaps is shown for two cases: (a) no applied flow and (b) applied flow dominates.

cases without applied flow [Fig. 1(b)], and where applied flow dominates [Fig. 1(c)].

Figure 2 shows how the final coverage of the area between the 75 μm gap varies as a function of the flow speed for an applied bias of 1 V. The coverage is defined as the fraction of the area of the gap that is occupied by gold in the micrographs of the final structures at the point where the electrochemical process self-terminates (as shown in the insets). As the flow speed increased, the final coverage between the gaps increased going from diffusion-limited deposition to ballistic deposition and by a flow speed of 1.44 mm/s, the gap is almost entirely filled.

III. COMPUTER SIMULATION

Studies of diffusion-limited aggregation (DLA) and branched growth in general [60–98] have provided insight

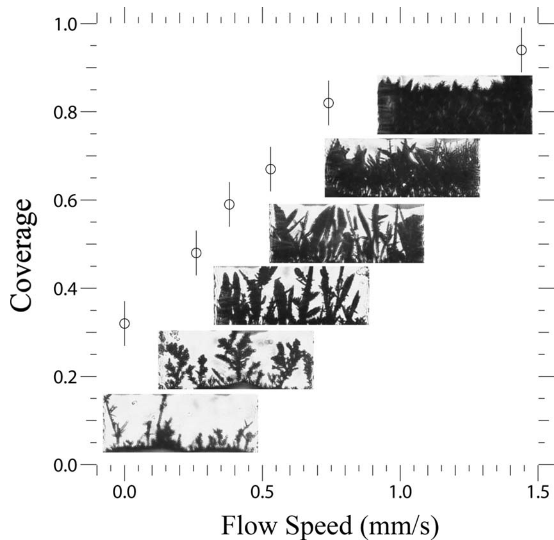

FIG. 2. Coverage vs flow speed. The insets show micrographs of the area in the electrode gaps (75 μm gaps and 200 μm wide).

into the electrodeposition process. The electrode geometry and low aspect ratio microchannel employed in the experiments presented here permit a two-dimensional (2D) representation. Consequently, a 2D model was developed to isolate the influences of diffusion, electric field ($\vec{E}$), and the applied flow in this process.

The simulation employed a random walk on a 2D lattice (210×210 points) with vertical flow and the probabilities of an ion at site (x,y) stepping to a nearest-neighbor site were given by

$$P_{x+1,y} = \frac{(P_D + P_E \Delta\phi_{x+1,y})}{P_0}, \tag{3}$$

$$P_{x-1,y} = \frac{(P_D + P_E \Delta\phi_{x-1,y})}{P_0}, \tag{4}$$

$$P_{x,y+1} = \frac{(P_D + P_E \Delta\phi_{x,y+1} - P_F)}{P_0}, \tag{5}$$

$$P_{x,y-1} = \frac{(P_D + P_E \Delta\phi_{x,y-1} + P_F)}{P_0}. \tag{6}$$

Where $\Delta\phi_{x+\Delta x,y+\Delta y}$ is defined as

$$\Delta\phi_{x+\Delta x,y+\Delta y} \equiv \phi_{x,y} - \phi_{x+\Delta x,y+\Delta y}. \tag{7}$$

The total probability is normalized to 1 by P_0, $\phi_{x,y}$ is the potential at site (x,y), and P_D, P_E, and P_F parametrize the effects of diffusion, $\vec{E}$, and the advection of the applied fluid flow, respectively. So that the strengths of the other parameters were always normalized relative to the contributions from the diffusion, $P_D=1$ was selected in all cases. Additionally, $\phi_{x,y}$ was normalized such that when $P_E=P_F$, they would make equal contributions to Eqs. (3)–(6) for electrodes in the initial configuration of parallel plates. Any probability less than 0 was set to 0. Each ion was initialized at a random site on the anode (top) and made a random walk based on these probabilities. If the ion contacted an occupied site, it adhered to the structure. Each time a particle adhered, $\phi_{x,y}$ was recalculated for the new geometry using the successive over relaxation method [99] to solve Laplace's equation and the process was repeated until the electrodes came into contact.

In Fig. 3, the results of several simulations are shown with the final coverage plotted versus the applied flow parameter, P_F. The cases of no contribution to the ion motion from the field ($P_E=0$, squares), weak contribution ($P_E=0.01$, circles), and strong contribution ($P_E=0.1$, triangles) are considered. The insets show examples of qualitative agreement between the model and the experiment. The left inset shows the results of a simulation with no flow and weak effective field ($P_F=0$, $P_E=0.01$). The right inset shows the final image of a simulation which included significant flow ($P_F=1.0$, $P_E=0.01$) and resembles the experimental micrographs for ballistic deposition. As the model does not take into account the three-dimensional nature of the experiment, the coverage is not as full as in the experimental case. When there is no flow in the simulation, the coverage clearly depends on the field as the electrophoresis driving the particles leads to denser

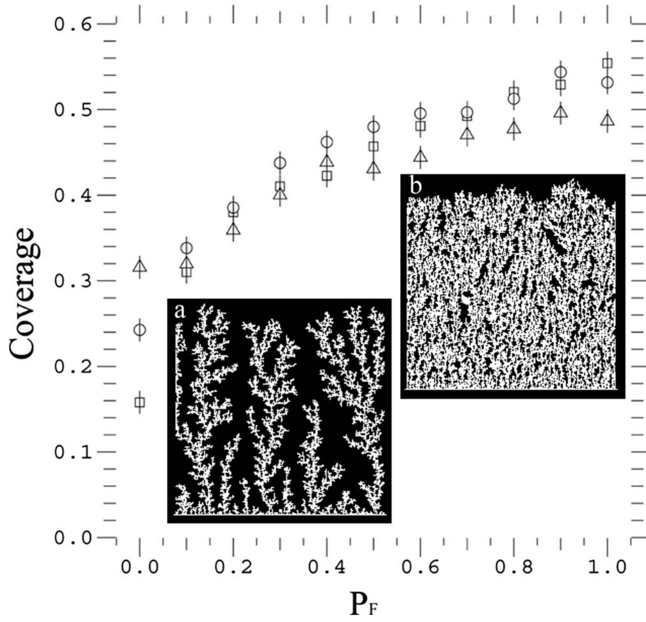

FIG. 3. Coverage vs P_F for P_E=0 (squares), P_E=0.01 (circles), and P_E=0.1 (triangles). The insets show are examples of final images for a small effective field (P_E=0.01) in two different case: (a) no applied flow (P_F=0) and (b) high applied flow (P_F=1.0).

structures. Even by P_F=0.1, flow begins to play an increasingly crucial role, and the coverage becomes less distinguishable between the different strength of the effective field. As the flow increases, the coverage increases, which is consistent with the results in these experiments and with the experiments on radial electrodeposition in larger systems [83,87]. For simulations at high flow velocities, the coverage is generally lower in the case of the strongest contribution from the field (P_E=1). In that case, it is the focusing effect of the stronger field that makes the electrode come to a sharper point which will be further examined in Sec. IV.

P_F is a dimensionless quantity that represents the strength of the applied flow normalized by the strength of diffusion in the model. An equivalent dimensionless quantity N_{Pe} (the Péclet number) is used to compare the advection due to the applied flow vs the rate of diffusion in the experiment,

$$N_{Pe} = Lv/D, \tag{8}$$

where L is a characteristic length scale (the gap size of 75 μm is selected), v is the mean flow velocity, and D is the diffusivity calculated using

$$D = \frac{k_B T}{6\pi\mu r}, \tag{9}$$

where T is the temperature (300 K), μ is the dynamic viscosity (1×10^{-3} N s/m^2), and r is the radius of Au (135 pm from Slater [100]). D is calculated to be 1.6×10^{-9} m^2/s. Using case shown in Fig. 2, the highest applied flow was 1.44 mm/s, resulting in N_{Pe}=67.5. Comparing ballistic deposition in the model and the experiment, for P_F=1, the applied flow strongly dominates as it does in this experimental case for N_{Pe}=67.5 which implies a scaling constant between these two dimensionless quantities on the order of 100. This means that since L was selected as 75 μm, 1 pixel in the simulation represents roughly 1 μm in the experiment.

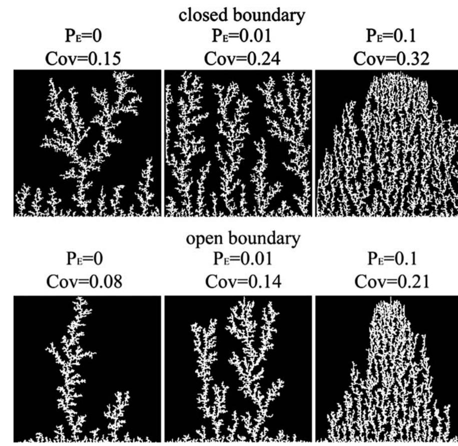

FIG. 4. Simulations with open and closed side boundaries while varying P_E leading to different final converages (Cov).

IV. CONTRIBUTIONS FROM $\vec{E}$ AND BOUNDARY CONDITIONS

In the original report of the self-terminated technique by Boussaad and Tao [46], tapering of the cathode was observed and attributed to a growth preference where $\vec{E}$ is highest. It was also suggested that $\vec{E}$ had a significant influence on self-terminated growth by Hu *et al.* [57]; however, no pronounced tapering was observed. An explanation of why focusing can be observed in environments where diffusion is the dominant mechanism is presented in Fig. 4. The effects of an open boundary (no lateral confinement of the Au ions), resembling the conditions in the experiment of Boussaad and Tao, are contrasted with a closed boundary model (lateral confinement of the Au ions) resembling the experiments presented here. The cases of P_E=0, P_E=0.01, and P_E=0.1 are presented with open and closed boundary conditions. In each case, the open boundary coverage was half of its closed boundary value with particles tending to accumulate in the middle or escape out the sides. In particular, the simulation of an open boundary and P_E=0 resemble the long branch growth seen by Hu *et al.* [57]. These results suggest that even in the absence of focusing induced by $\vec{E}$, an open boundary condition can result in the tapering effects previously attributed to the electric field. In contrast, lateral microconfinement results in more uniform growth under similar growth conditions.

Screening effects at the electrode surfaces are expected to effectively reduce $\vec{E}$. The Debye length (λ_D) is the characteristic length scale over which ion charge is screened in the Debye-Hückel model

$$\lambda_D = \sqrt{\frac{\epsilon_0 \epsilon_r R T}{2F^2 C_0}}, \tag{10}$$

where ϵ_0 is the permittivity of free space, ϵ_r is the dielectric constant of water, R is the ideal gas constant, T is the tem-

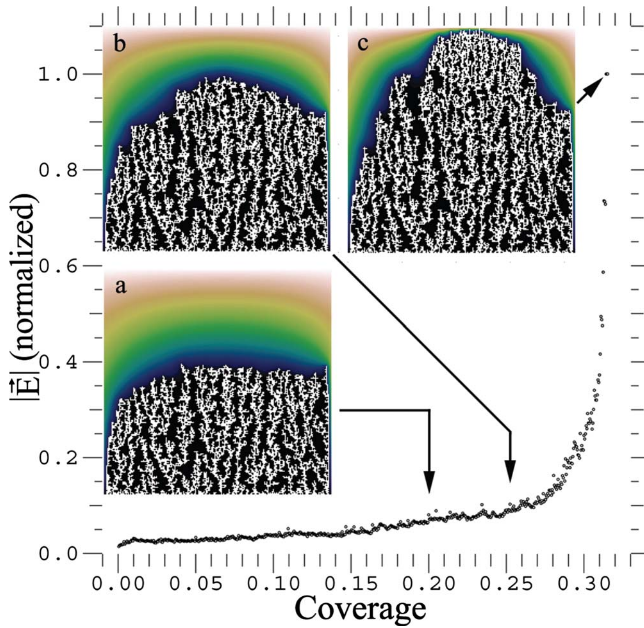

FIG. 5. (Color online) Maximum normalized $|\vec{E}|$ vs coverage during simulated cathode growth ($P_F=0$, $P_E=0.1$). Panels a–c (corresponding to coverages of 0.200, 0.252, and 0.316, respectively) show accumulated particles in white and equipotentials of $\phi_{x,y}$ in color as the simulation progressed.

perature, F is the Faraday constant, and C_0 is the concentration of HCl ($0.2M$). In this case, $\lambda_D=0.7$ nm, which means that $\vec{E}$ should be strongly screened out across the electrodes as opposed to driving the morphology as previously suggested. With λ_D being so small, the mechanism for focused growth is not expected to be significant in the experiment except on a smaller length scale or for lower concentrations.

Future work with low concentrations or at smaller scales could be used to verify the dynamics of focused growth where screening does not play as large a role. Even with a closed boundary, a strong field ($P_E=0.1$) can induce tapering as suggested. Consequently, the dynamic effects of $\vec{E}$ during deposition were investigated in the simulation. Figure 5 shows the maximum value of $|\vec{E}|$ as a function of coverage (the fraction of the total area occupied by particles between the electrodes). $\vec{E}$ was calculated from the middle region of 170×210 points to minimize boundary artifacts, and was normalized such that $|\vec{E}|=1$ when the electrodes were within 1 lattice spacing from each other. Panels a–c show a progression of growth coverages (0.200, 0.252, and 0.316, respectively) with accumulated particles in white, and color contours corresponding to the equipotentials of $\phi_{x,y}$. In Fig. 5(a), the overall front of the cathode was only slightly rounded, but curvature of the potential indicates that further particles would be focused toward the middle of the channel as they approached the cathode. In Fig. 5(b) (coverage of 0.252), the focusing potential resulted in the curvature becoming more pronounced as particles tended to accumulate in regions of higher $\vec{E}$. Figure 5(c) shows increased particle density (coverage of 0.316) and curvature in response to the increased electric field strength as the space between the electrodes decreases.

V. CONCLUDING REMARKS

Self-terminating electrodeposition with microfluidic flow yields some interesting results and is a useful tool with which to independently manipulate electrodeposition without affecting electrochemical processes. Microfluidics has a host of sophisticated techniques for physics and chemistry applications which promises to extend future work on this subject [101,102]. Within the microfluidic channels branching growth was observed between the electrodes during electrodeposition without flow. A dense macroscopic structure dominated by applied flow was formed during higher flow rates on the order of mm/s distinct from any structures reported in previous work on self-terminated electrodeposition, and in both experiment and simulation, the applied flow dramatically increased the coverage between the electrodes. In the computer simulations of self-terminated growth, varying $\vec{E}$ and choosing open or closed boundaries can account for the differences in tapered and untapered structures. This is in contrast to a highly screened system based solely on a calculation of λ_D which would imply that $\vec{E}$ would only be relevant on small length scales.

ACKNOWLEDGMENTS

This work was funded by grants from CFI, BCKDF, and NSERC. We would also like to acknowledge Dr. Viatcheslav Berejnov for his assistance with the microfluidic fabrication.

[1] J. I. Pascual, J. Méndez, J. Gómez-Herrero, A. M. Baró, N. García, and V. T. Binh, Phys. Rev. Lett. **71**, 1852 (1993).
[2] L. Olesen, E. Laegsgaard, I. Stensgaard, F. Besenbacher, J. Schiotz, P. Stoltze, K. W. Jacobsen, and J. K. Norskov, Phys. Rev. Lett. **72**, 2251 (1994).
[3] J. I. Pascual, J. Méndez, J. Gómez-Herrero, A. M. Baró, N. García, U. Landman, W. D. Luedtke, E. N. Bogachek, and H.-P. Cheng, Science **267**, 1793 (1995).
[4] M. Brandbyge, J. Schiøtz, M. R. Sørensen, P. Stoltze, K. W. Jacobsen, J. K. Nørskov, L. Olesen, E. Laegsgaard, I. Stensgaard, and F. Besenbacher, Phys. Rev. B **52**, 8499 (1995).
[5] N. Agrait, G. Rubio, and S. Vieira, Phys. Rev. Lett. **74**, 3995 (1995).
[6] Z. Gai, Y. He, H. Yu, and W. S. Yang, Phys. Rev. B **53**, 1042 (1996).
[7] A. Stalder and U. Durig, Appl. Phys. Lett. **68**, 637 (1996).
[8] G. Rubio, N. Agrait, and S. Vieira, Phys. Rev. Lett. **76**, 2302 (1996).
[9] C. Sirvent, J. G. Rodrigo, S. Vieira, L. Jurczyszyn, N. Mingo, and F. Flores, Phys. Rev. B **53**, 16086 (1997).
[10] J. L. Costa-Krämer, Phys. Rev. B **55**, R4875 (1996).
[11] G. Cross, A. Schirmeisen, A. Stalder, P. Grütter, M. Tschudy,

and U. Dürig, Phys. Rev. Lett. **80**, 4685 (1998).
[12] T. Junno, S.-B. Carlsson, H. Xi, L. Montelius, and L. Samuelson, Appl. Phys. Lett. **72**, 548 (1998).
[13] A. I. Yanson, G. Rubio Bollinger, H. E. van den Brom, N. Agraït, and J. M. van Ruitenbeek, Nature (London) **395**, 783 (1998).
[14] C. Untiedt, G. R. Bollinger, S. Vieira, and N. Agrait, Phys. Rev. B **62**, 9962 (2000).
[15] D. Erts, H. Olin, L. Ryen, E. Olsson, and A. Thölén, Phys. Rev. B **61**, 12725 (2000).
[16] K. Hansen, S. K. Nielsen, M. Brandbyge, E. Lægsgaard, I. Stensgaard, and F. Besenbacher, Appl. Phys. Lett. **77**, 708 (2000).
[17] J. I. Mizobata, A. Fujii, S. Kurokawa, and A. Sakai, Phys. Rev. B **68**, 155428 (2003).
[18] J. M. Krans, C. J. Muller, I. K. Yanson, T. C. M. Govaert, R. Hesper, and J. M. van Ruitenbeek, Phys. Rev. B **48**, 14721 (1993).
[19] J. M. Krans, J. M. van Ruitenbeek, V. V. Fisun, I. K. Yanson, and L. J. de Jongh, Nature (London) **375**, 767 (1995).
[20] C. Zhou, C. J. Muller, M. R. Deshpande, J. W. Sleight, and M. A. Reed, Appl. Phys. Lett. **67**, 1160 (1995).
[21] C. J. Muller, J. M. Krans, T. N. Todorov, and M. A. Reed, Phys. Rev. B **53**, 1022 (1996).
[22] E. Scheer, P. Joyez, D. Esteve, C. Urbina, and M. H. Devoret, Phys. Rev. Lett. **78**, 3535 (1997).
[23] E. Scheer, N. Agrait, J. C. Cuevas, A. L. Yeyati, B. Ludoph, A. Martin-Rodero, G. R. Bollinger, J. M. van Ruitenbeek, and C. Urbina, Nature (London) **394**, 154 (1998).
[24] H. Mehrez, A. Wlasenko, B. Larade, J. Taylor, P. Grütter, and H. Guo, Phys. Rev. B **65**, 195419 (2002).
[25] C. Untiedt, D. M. T. Dekker, D. Djukic, and J. M. van Ruitenbeek, Phys. Rev. B **69**, 081401(R) (2004).
[26] A. Halbritter, S. Csonka, G. Mihaly, O. I. Shklyarevskii, S. Speller, and H. vanKempen, Phys. Rev. B **69**, 121411(R) (2004).
[27] E. Scheer, P. Konrad, C. Bacca, A. Mayer-Gindner, H. v. Löhneysen, M. Häfner, and J. C. Cuevas, Phys. Rev. B **74**, 205430 (2006).
[28] Y. Kondo and K. Takayanagi, Phys. Rev. Lett. **79**, 3455 (1997).
[29] H. Ohnishi, Y. Kondo, and K. Takayanagi, Nature (London) **395**, 780 (1998).
[30] P. Steinmann and J. M. R. Weaver, J. Vac. Sci. Technol. B **22**, 3178 (2004).
[31] P. Steinmann and J. M. R. Weaver, Appl. Phys. Lett. **86**, 063104 (2005).
[32] M. Yoshida, Y. Oshima, and K. Takayanagi, Appl. Phys. Lett. **87**, 103104 (2005).
[33] R. Negishi, T. Hasegawa, K. Terabe, M. Aono, T. Ebihara, H. Tanaka, and T. Ogawa, Appl. Phys. Lett. **88**, 223111 (2006).
[34] M. D. Fischbein and M. Drndić, Appl. Phys. Lett. **88**, 063116 (2006).
[35] M. D. Fischbein and M. Drndić, Nano Lett. **7**, 1329 (2007).
[36] H. Park, A. K. L. Lim, A. P. Alivisatos, J. Park, and P. L. McEuen, Appl. Phys. Lett. **75**, 301 (1999).
[37] J. Park *et al.*, Nature (London) **417**, 722 (2002).
[38] A. Anaya, A. L. Korotkov, M. Bowman, J. Waddell, and D. Davidovic, J. Appl. Phys. **93**, 3501 (2003).
[39] A. Anaya, M. Bowman, and D. Davidovic, Phys. Rev. Lett. **93**, 246604 (2004).
[40] M. Bowman, A. Anaya, A. L. Korotkov, and D. Davidović, Phys. Rev. B **69**, 205405 (2004).
[41] A. Anaya, M. Bowman, A. L. Korotkov, and D. Davidović, Phys. Rev. B **72**, 035452 (2005).
[42] K. O'Neill, E. A. Osorio, and H. S. J. van der Zant, Appl. Phys. Lett. **90**, 133109 (2007).
[43] C. Z. Li and N. J. Tao, Appl. Phys. Lett. **72**, 894 (1998).
[44] A. F. Morpurgo, C. M. Marcus, and D. B. Robinson, Appl. Phys. Lett. **74**, 2084 (1999).
[45] C. Z. Li, H. X. He, A. Bogozi, J. S. Bunch, and N. J. Tao, Appl. Phys. Lett. **76**, 1333 (2000).
[46] S. Boussaad and N. J. Tao, Appl. Phys. Lett. **80**, 2398 (2002).
[47] F. Elhoussine, S. Mátéfi-Tempfli, A. Encinas, and L. Piraux, Appl. Phys. Lett. **81**, 1681 (2002).
[48] F. Elhoussine, A. Encinas, S. Mátéfi-Tempfli, and L. Piraux, J. Appl. Phys. **93**, 8567 (2003).
[49] S. Boussaad, B. Xu, L. Nagahara, I. Amiani, W. Schmickler, R. Tsui, and N. J. Tao, J. Chem. Phys. **118**, 8891 (2003).
[50] L. H. Yu and D. Natelson, Appl. Phys. Lett. **82**, 2332 (2003).
[51] L. H. Yu and D. Natelson, Phys. Rev. B **68**, 113407 (2003).
[52] S. Z. Hua and H. D. Chopra, Phys. Rev. B **67**, 060401(R) (2003).
[53] E. B. Svedberg, J. J. Mallett, H. Ettedgui, L. Gan, P. J. Chen, A. J. Shapiro, T. P. Moffat, and W. F. Egelhoff, Jr., Appl. Phys. Lett. **84**, 236 (2004).
[54] F. Chen, Q. Qing, L. Ren, Z. Wu, and Z. Liu, Appl. Phys. Lett. **86**, 123105 (2005).
[55] P. Castle and P. Bohn, Anal. Chem. **77**, 243 (2005).
[56] G. Mészáros, S. Kronholz, S. Karthäuser, D. Mayer, and T. Wandlowski, Appl. Phys. A: Mater. Sci. Process. **87**, 569 (2007).
[57] Y. Hu, N. Pan, K. Zhang, Z. Wang, H. Hu, and X. Wang, Phys. Status Solidi **204**, 3398 (2007) a.
[58] G. Z. Xiaodong Dong, Yong Xia, and B. Zhang, Nanotechnology **18**, 395502 (2007).
[59] J. C. McDonald, D. C. Duffy, J. R. Anderson, D. T. Chiu, H. Wu, O. J. A. Schueller, and G. M. Whitesides, Electrophoresis **21**, 27 (2000).
[60] T. A. Witten and L. M. Sander, Phys. Rev. Lett. **47**, 1400 (1981).
[61] T. A. Witten and L. M. Sander, Phys. Rev. B **27**, 5686 (1983).
[62] M. Matsushita, M. Sano, Y. Hayakawa, H. Honjo, and Y. Sawada, Phys. Rev. Lett. **53**, 286 (1984).
[63] D. Grier, E. Ben-Jacob, R. Clarke, and L. M. Sander, Phys. Rev. Lett. **56**, 1264 (1986).
[64] Y. Sawada, A. Dougherty, and J. P. Gollub, Phys. Rev. Lett. **56**, 1260 (1986).
[65] E. Ben-Jacob, G. Deutscher, P. Garik, N. D. Goldenfeld, and Y. Lareah, Phys. Rev. Lett. **57**, 1903 (1986).
[66] F. Argoul, A. Arneodo, G. Grasseau, and H. L. Swinney, Phys. Rev. Lett. **61**, 2558 (1988).
[67] S. E. May and J. V. Maher, Phys. Rev. A **40**, 1723 (1989).
[68] P. Garik, D. Barkey, E. Ben-Jacob, E. Bochner, N. Broxholm, B. Miller, B. Orr, and R. Zamir, Phys. Rev. Lett. **62**, 2703 (1989).
[69] G. L. M. K. S. Kahanda and M. Tomkiewicz, J. Electrochem. Soc. **136**, 1497 (1989).
[70] D. B. Hibbert, J. R. Melrose, and R. C. Ball, Proc. R. Soc. London, Ser. A **423**, 149 (1989).

[71] J. R. Melrose and D. B. Hibbert, Phys. Rev. A **40**, 1727 (1989).
[72] J. R. Melrose, D. B. Hibbert, and R. C. Ball, Phys. Rev. Lett. **65**, 3009 (1990).
[73] E. Ben-Jacob and P. Garik, Nature (London) **343**, 523 (1990).
[74] C. Yeung and D. Jasnow, Phys. Rev. A **41**, 891 (1990).
[75] Y. Lereah, G. Deutscher, and E. Grünbaum, Phys. Rev. A **44**, 8316 (1991).
[76] P. P. Trigueros, J. Claret, F. Mas, and F. Sagues, J. Electroanal. Chem. **312**, 219 (1991).
[77] V. Fleury, M. Rosso, and J. N. Chazalviel, Phys. Rev. A **43**, 6908 (1991).
[78] V. Fleury, M. Rosso, J.-N. Chazalviel, and B. Sapoval, Phys. Rev. A **44**, 6693 (1991).
[79] H. Honjo and S. Ohta, Phys. Rev. A **45**, R8332 (1992).
[80] J. R. Melrose, Europhys. Lett. **19**, 51 (1992).
[81] D. Barkey, P. Garik, E. Ben-Jacob, B. Miller, and B. Orr, J. Electrochem. Soc. **139**, 1044 (1992).
[82] D. G. Grier and D. Mueth, Phys. Rev. E **48**, 3841 (1993).
[83] L. López-Tomàs, J. Claret, and F. Sagués, Phys. Rev. Lett. **71**, 4373 (1993).
[84] J. Erlebacher, P. C. Searson, and K. Sieradzki, Phys. Rev. Lett. **71**, 3311 (1993).
[85] A. Kuhn and F. Argoul, Phys. Rev. E **49**, 4298 (1994).
[86] J. M. Huth, H. L. Swinney, W. D. McCormick, A. Kuhn, and F. Argoul, Phys. Rev. E **51**, 3444 (1995).
[87] S. Fautrat and P. Mills, Phys. Rev. E **53**, 4990 (1996).
[88] V. Fleury and D. Barkey, Physica A **233**, 730 (1996).
[89] J. K. Lin and D. G. Grier, Phys. Rev. E **54**, 2690 (1996).
[90] O. Zik and E. Moses, Phys. Rev. E **53**, 1760 (1996).
[91] C. Léger, J. Elezgaray, and F. Argoul, Phys. Rev. Lett. **78**, 5010 (1997).
[92] M.-Q. Lopez-Salvans, F. Sagues, J. Claret, and J. Bassas, J. Electroanal. Chem. **421**, 205 (1997).
[93] M.-Q. Lòpez-Salvans, F. Sagués, J. Claret, and J. Bassas, Phys. Rev. E **56**, 6869 (1997).
[94] F. Oberholtzer, D. Barkey, and Q. Wu, Phys. Rev. E **57**, 6955 (1998).
[95] M. Castro, R. Cuerno, A. Sánchez, and F. Domínguez-Adame, Phys. Rev. E **62**, 161 (2000).
[96] H. Mizuseki and Y. Kawazoe, J. Appl. Phys. **87**, 4611 (2000).
[97] G. Gonzalez, G. Marshall, F. Molina, and S. Dengra, Phys. Rev. E **65**, 051607 (2002).
[98] G. Marshall, E. Mocskos, F. V. Molina, and S. Dengra, Phys. Rev. E **68**, 021607 (2003).
[99] W. Cheney and D. Kincaid, *Numerical Mathematics and Computing*, 5th ed. (Brooks/Cole, Belmont, MA, 2004).
[100] J. C. Slater and A. Russek, Am. J. Phys. **32**, 65 (1964).
[101] T. M. Squires and S. R. Quake, Rev. Mod. Phys. **77**, 977 (2005).
[102] G. M. Whitesides, Nature (London) **442**, 368 (2006).